Identification of safety hazards and operating conditions of the low-floor tram with independently rotating wheels with various drive control algorithms

Robert Konowrocki[a,*], Dariusz Kalinowski[a,b], Tomasz Szolc[a], Artur Marczewski[b]

[a]Institute of Fundamental Technological Research, Polish Academy of Sciences, ul. Pawińskiego 5b, 02-106 Warsaw, Poland
[b]PESA Bydgoszcz SA, ul. Zygmunta Augusta 11, 85-082 Bydgoszcz, Poland

Highlights

- Bogies with independently rotating wheels increase travel comfort.

- System of independently rotating wheels (IRW) reducing the value of wheel-rail forces.

- Higher efficiency of tram drive control through additional braking.

- New geometry of simulational test track for light rail vehicles (LRVs).

- New control of an innovative drive with a crank axle for light rail vehicles (LRVs).

Abstract

The aim of the article is to develop a method for the analysis of tram dynamics related to safety during operation. To achieve this, a mathematical model of the vehicle represented by a multibody simulation MBS system is used. Models of tram with a classic and innovative drive, based on a system of independently rotating wheels on crank axles are analyzed. A new configuration of an innovative drive control of the considered vehicle with the use of braking of independent wheels is proposed. A new geometry of test track is presented. During numerical investigation the values of 'Y' leading forces of tram wheels with the considered innovative drive proved to be lower than in the corresponding vehicle with standard wheelsets. It has been demonstrated that the active control systems are of key importance and should be applied in such innovative tram drives.

Keywords

maintenance of safety, reliability of trams, derailment of tramcar, numerical tests, drive with independently rotating wheel, SIMPACK Rail.

1. Introduction

In years 2014 to 2020, the European transport infrastructure began to change. This transformation was triggered by introducing common EU policy aimed at effective, safe and economically efficient movement of people and goods as well as reduction of environmental pollution as a part of a new EU sustainable development transport policy. Poland is known as the EU member state that, within the framework of the operational program Infrastructure and Environment, submitted the largest number of applications by the year 2020 (the total number of 178). In the period 2014-2020 (fig. 1) the projects were financed from the European Structural and Investment Funds (ESIF), the the Cohesion Fund (CF) and the European Regional Development Fund (ERDF). Great amount of submitted applications concerned the design and construction of new public transport infrastructure as well as modernization of the existing one, including the tram rolling stock [47, 33]. In Poland, very good examples of projects financed from the ESIF were tram projects approved for implementation, e.g. "Construction of a tram line along Kujawska street, from Kujawskie roundabout to Bernardyńskie roundabout, along with the extension of road network, reconstruction of rail transport system and rolling stock purchase in Bydgoszcz" (cost EUR 86 579 938), "Reconstruc-

tion of tramway tracks in Szczecin, stage II" (cost EUR 77 014 409), "Construction of a tramline to Gocław in Warsaw with the rolling stock purchase" (cost EUR 91 019 802), "Comprehensive integration programme for the low-emission public transport system in Łódź Metropolitan Area, including the purchase of means of transport for service on the W-Z (East-West) and other transport routes, as well as modernisation of tram depots in Łódź" (cost EUR 151 759 547).

The above-mentioned facts prove, that there is the necessity of an intensive development in the area of tram transport, and greater commitment to conduct research and tests related to the improvement of reliability, safety and maintenance of tram fleet and its infrastructure.

2. Modern stock of light rail vehicles

One of the above-mentioned methods to develop and increase the efficiency of the public transport, especially in urban area, are modern tram vehicles. One category of the Light Rail Vehicles (LRV) [9] are low-floor trams which contributed to the increase of transport efficiency and passenger comfort improvement. By reducing the total time spent by the vehicle at tram stop and facilitating boarding and unboarding of passengers, the low-floor trams – compared to con-

(*) Corresponding author.
E-mail addresses: R. Konowrocki - rkonow@ippt.pan.pl, D. Kalinowski - dariusz.kalinowski@pesa.pl, T. Szolc - tszolc@ippt.pan.pl,
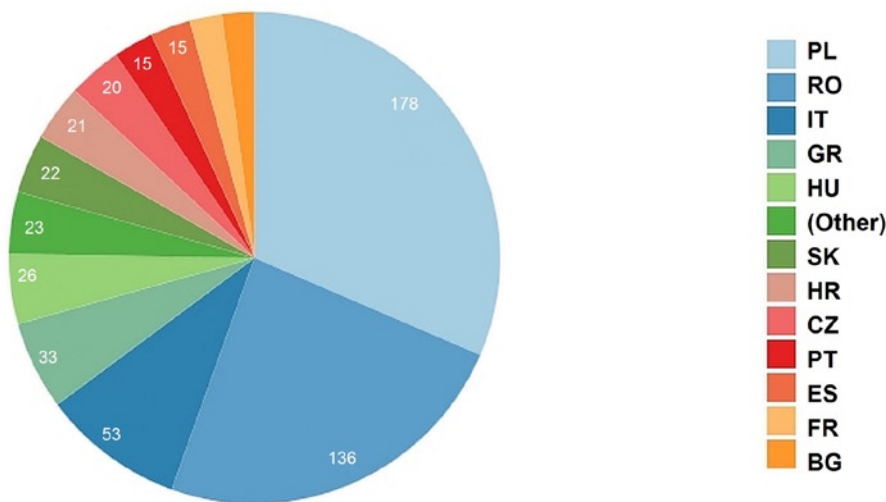A. Marczewski - artur.marczewski@pesa.pl

Fig. 1. The number of applications submitted by the EU member states for the development of transport infrastructure; applications under the ESIF 2014-2020 ERDF CF projects [46]

ventional trams [39] - affected the growth of public transport commuters number. The very important feature of low-floor vehicles is an easy access for People with Reduced Mobility (PRM), e.g. traveling in wheelchairs, or parents with baby strollers. Due to new passenger mobility requirements [13] a fundamental change in production technology of tram vehicles has been introduced. Greater internal volume of tram bodies as well as lowering and flattening of the floor [25] were expected. Allocation of equipment on tram roof and crucial redesign of car bodies structure, as well as independently rotating wheels (IRW) (Fig. 2) [5] were implemented. Operational introduction of trams with independently rotating wheels allowed lowering the floor height relative to the level of rail head along the entire length of the tram without lifting the level above the bogies [15]. Examplary constructions of bogies with IRW are presented in papers [25, 23]. Such a wheelset has wheels mounted on a common axle by means of bearing system which enables independent rotation of wheels. A continuous development of IRW trams could have been observed at international fairs where tram producers presented their new vehicle designs: PESA Jazz, Siemens Avenio, Alstom Citadis and Škoda Forcity Plus. The Hyundai Rotem company is on the way to finish their work on an IRW tram, capable of traveling on curves with radius R = 15 m. The vehicle is expected to be equipped with individual motor torque control and hydraulic actuators that reduce the angle of the wheelset of the bogie running on rail. Unfortunately, the research results are not commonly available. The facts presented above indicate that the research topics discussed in this article are still current, investigated and important for the transport development both on Polish and international level.

As opposed to vehicles with standard wheelsets, the application of independently rotating wheels entails direct control of wheel propulsions [4, 18]. Such control is required due to the fact that in specific conditions the IRW bogie can be characterized by worse kinematic and dynamic properties compared to standard solution with a rigid axle that couples the angular velocities of both wheels [38, 29]. As a result of independence from the velocity constraints mentioned above, wheelsets with independently rotating wheels present difficulties in self-centering, e.g. after leaving the curve arc [2, 30]. Such behaviour has been proven in many studies, e.g. [5, 7]. The quality of operating conditions and maintenance of light tram vehicles could be significantly reduced thanks to such behaviour of a tram [19]. The occurrence of the non-centering of IRW wheelsets also reduces safety against derailment by increasing the Y guiding force [38]. This results in an increase of the Y / Q derailment ratio and a greater D_z wheel lift that consequently enhances the probability of a vehicle derailment [26, 14]. Co-authors of this publication developed their own method of determining the safety level against tram derailment; their assumptions are presented in article [19]. So far none of the methods of determining the safety level against tram derailment has been standardized. The analyses of derailment safety were the subject of many publications [37, 11]. However, it should be emphasized that the quasi-static ride of a tram on a curve with a specified twist is a conservative approach to the simulation derailment analysis. Due to tram reduced velocity the conditions of such ride are particularly disadvantageous since in case of smaller velocity the dynamic friction coefficient is greater at smaller skids [24] and the curve radius of the railway track is smaller than in case of standard railway lines [46]. The motor bogies of IRW trams are equipped with motorized wheelsets (Fig. 2), each one driving one of the wheels. The difficulty in proper steering and synchronization of the system of independently rotating wheels is the main drawback of the solution in question. The existing algorithms [5, 18] allow to control such system in model conditions with a standard set of rail arrangements. However, due to different state of tracks and tram infrastructure in many municipalities [44], it is very important to adapt such type of tram drive systems to different conditions. Therefore an analysis was made to check the impact of the track gauge change on vehicle dynamics with various control configurations, ensuring right tram safety conditions. By addressing this topic the present article partially develops and supplements the subjects presented by the authors of the works [2, 12, 43]. Based on obtained results of numerical analysis, numerous researchers [8] recommended active steering and optimal control strategies for independently rotating wheels. Unfortunately, experimental validations did not take place in their case. As a result of experimental research it was proved [28] that - compared to standard wheelset - active control of the motors wheelset with independently rotating wheels gives a better stability of the vehicle. Authors of [29] showed that the application of an indirect method of controlling induction motors through the orientation of the stator magnetic field is sufficient, both in terms of response and controllability of the rail vehicle. In terms of wheel steering, braking was not taken into account in these papers.

Fig. 2. Low-floor tram vehicle motor bogie with cranked axles [50,16]

So far the approach of controlling the propulsion of trams with independently rotating wheels with the braking possibility has not been utilized. Therefore authors of this paper made attempt to include braking into approach. The main example of the execution and application possibilities of the propulsion control configuration proposed in this article is the algorithm consisting of a simultaneous indirect torque and flux control of the drive motor [4, 36]. This approach enables smooth setting of the driving torque and the braking torque of motors. In this way electrodynamic braking is achieved in the entire rotational speed range [50]. For a given vehicle velocity the braking torque value can be the same as the driving torque value. The feature of asynchronous motors applied in tram vehicles was implemented by the authors of this paper for the control variant with the option of braking a given wheel discussed in the article.

This paper presents the results of studies of the implementation of several drive control algorithms in a tram as well as the results of an analysis carried out on their basis of these studies. Additionally, the impact of this control on the track guiding force and on safety against derailment is presented. A novelty in the presented method is the implementation of braking procedure while riding in small radius curves. The results of the considered algorithms of controlling the propulsion of independently rotating bogie wheels were compared with the results of standard tram wheel sets. In addition to the above, the authors proposed a new track geometry with an additional twist for tram tests which is an alternative to the the geometry presented in the EN 14363:2016 standard [10], used for extra-urban passenger rail vehicles and freight vehicles. The results of the analysis presented in this article are of great importance for the development of expertise and innovation in the field of transport.

3. Theoretical studies of a tramway vehicle dynamics

3.1. Description of mathematical model

The model of a tramway vehicle consists of non-deformable bodies with given masses and moments of inertia that represent the dynamic properties of its individual elements. Rigid solids representing the inertial properties of the vehicle body were connected with analogous solids corresponding to bogie frames by means of massless elastic-damping elements replacing the secondary suspension.

On the other hand, crank axles with railway wheels were attached to the rigid bodies representing bogie frames by means of massless elastic-damping elements replacing the primary suspension. The rigid bodies corresponding to the individual carbodies of the tramway vehicle body were interconnected by means of massless connectors. The interaction between the vehicle and railway track as

elastic normal forces and tangential friction forces in the wheel-rail contact zone were described. The presented approach to building a vehicle model is called multibody simulation method (MBS) and is utilised by many authors investigating the interaction and dynamics of railway vehicles [1, 37, 38]. In order to determine the effect of a control algorithm of vehicle drive torque on their dynamic behaviour, the considered model based on the above-described method was prepared.

The structure of the modeled tram is shown in Figure 3. The vehicle model under consideration consists of five carbodies marked with the letters A-E and is based on three bogies - two motor-bogies MB and one trailer-bogie TB. Adjacent carbodies are articulated. Their lower joint constitutes a spherical joint. The upper joint also uses ball joints. However, in case of an upper link between the carbodies C and D, a Panhard rod is installed. This allows the carbodies to rotate relative to the transverse y and vertical z axes of global coordinate. The angular displacements of the carbody relative to each other are denoted by the symbol β for rotation about the y axis and the symbol γ for rotation about the z axis.
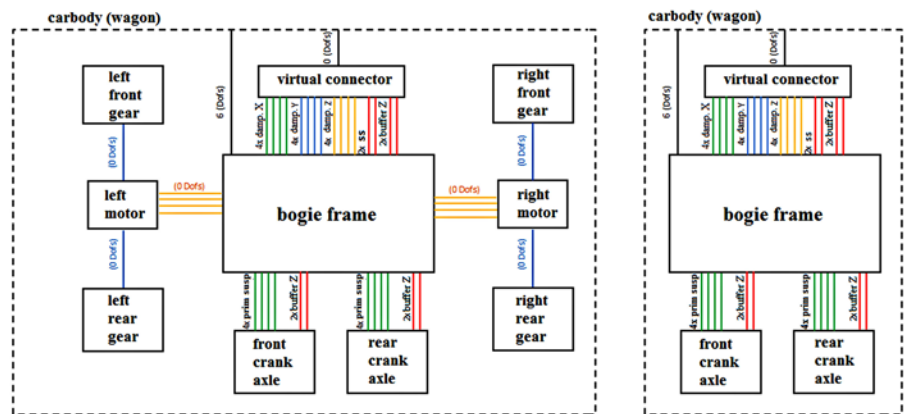

Fig. 4. Topology of the motor-bogie and trailer-bogie of the tram under consideration

The tram model considered in this paper has been divided into three basic elements, which are: vehicle parts (bodies), bogie frames and wheelsets with cranked axles. The elements of the considered vehicle represent rigid bodies with six degrees of freedom (DOF) relative to the stationary Cartesian inertial Oxyz coordinate system associated with the track (Fig. 3). The degrees of freedom define the lateral displacement y_{nk}, vertical displacement z_{nk}, longitudinal displacement x_{nk}, attack angle φ_{nk}, hunting angle θ_{nk}, and galloping angle ϕ_{nk}, where k takes the value $k=1\div5$, and n – corresponds to the number of vehicle units. The bogie frame is also replaced by a rigid body with five degrees of freedom that describes the lateral displacement y_{rj}, vertical displacement z_{rj}, attack angle φ_{rj}, hunting angle θ_{rj}, and galloping angle ϕ_{rj} (Fig. 3). In this case, the index takes values $j=1\div3$. The model of each wheelset is a subsystem consisting of 3 rigid bodies, a cranked axle to which two rigid discs representing railway wheels are rotatably attached (Fig. 4). Lateral displacements of the wheelset are marked with the symbol y_i, attack angle φ_i, and rolling angel of wheel ϕ_{Li}, ϕ_{Ri}, different for left and right wheel. In the description of these symbols, the index i corresponds to the individual wheelsets, taking the values $i=1\div6$.

The dynamics of the mathematical model of the considered vehicle was described by the second order ordinary differential equations. Assuming that the oscillations of the individual rigid bodies of the model relative to the reference system are small, their movement can be described by means of a linearized system of equations. This system
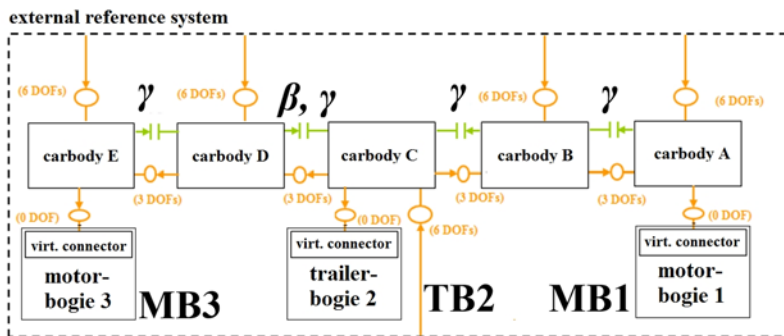

Fig. 3. Topology of considered tram model with indication of interconnections and degrees of freedom
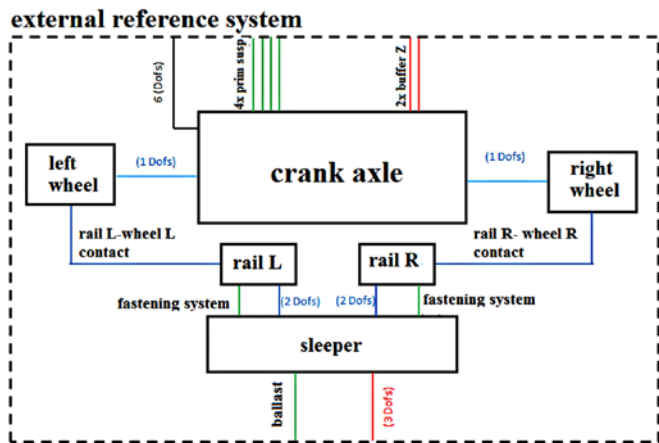
Fig. 5. Topology of a cranked axle with independently rotating wheels and railway track

of equation in the following matrix-operational form is presented below (1):

$$\left[\mathbf{M}\frac{d^2}{dt^2} + \mathbf{D}\frac{d}{dt} + \mathbf{K}\right] \cdot \mathbf{q} = \mathbf{F} + \mathbf{W} \tag{1}$$

where: $\mathbf{M}_{NxN}$ dentotes the mass matrix, $\mathbf{D}_{NxN}$ is the damping matrix, $\mathbf{K}_{NxN}$ describes the stiffness matrix, and $\mathbf{q}_{Nxp} = \{ y_i, z_i, \varphi_i, \phi_i, y_{rj}, z_{rj}, \varphi_{rj}, \theta_{rj}, \phi_{rj}, y_{nk}, z_{nk}, \varphi_{nk}, \theta_{nk}, \phi_{nk}, ...\}^T$ is the vector of generalized coordinates, $\mathbf{F}$ is the vector of contact forces, $\mathbf{W}$ denotes the vector of forces from kinematic excitations caused by e.g. unevenness of the railway tracks, d/dt is the differential operator, and N denotes the number of degrees of freedom of the considered model. The number of degrees of freedom in the vehicle model under analysis was 127. As a result of the Newmark method, the system of motion equations (1) is reduced to a system of linear algebraic equations which are numerically solved with the time step $\Delta t = 0.005$ s.

3.2. Wheel-rail contact model

The numerical procedures presented below have been integrated with the above-described mathematical model of a tramway vehicle, enabling the determination of the forces of dynamic interaction in the wheel-rail contact zones of the vehicle. These procedures are based on the Polach contact model [41]. In the approach used, the contact forces induced by micro-slips F_ξ and F_η are determined by the tangential force F acting in the contact zone, caused by the longitudinal and transverse micro-slip v_ξ, v_η, as well as by the transverse force $F_{\eta S}$ which is caused by the presence of a spin moment

S resulting from the usually conical tread of the wheel profile of the considered railway vehicle. Mathematically, it can be described by equations (2), (3) and (4) as follows:

$$v_C = \sqrt{{v_\xi}^2 + \left(v_\eta + \varphi \cdot a\right)^2} , \tag{2}$$

$$F_\xi = F\frac{v_\xi}{v_C} , \tag{3}$$

$$F_\eta = F\frac{v_\eta}{v_C} + F_{\eta S}\frac{\varphi}{v_C} , \tag{4}$$

where: F denotes the tangential contact force caused by the longitudinal v_ξ and transverse v_η micro-slip, v_C is the modified translational micro-slip that takes into account the effect of the spin-induced spin torque ϕ on the arm of the semi-axis a, and the contact zone ellipse (in the longitudinal direction), $F_{\eta S}$ is the transverse tangential force caused by the spin torque S. The algorithm [41] used to determine the contact forces requires the introduction of micro-slips v_ξ, v_η and F normal contact force N, semi-axes a and b of the contact zone ellipse, combined transverse modulus of the wheel and the rail G, friction coefficient μ and creep force Kalker's coefficients f_{11}, f_{12}, f_{22}, f_{33} expressed in terms of equations (5) [20].

$$\begin{aligned} f_{11} &= (ab)\, Gc_{11}, \quad f_{23} = (ab)^{3/2}\, Gc_{23}, \\ f_{22} &= (a/b)^2\, Gc_{22}, \quad f_{33} = (ab)^2\, Gc_{33}, \end{aligned} \tag{5}$$
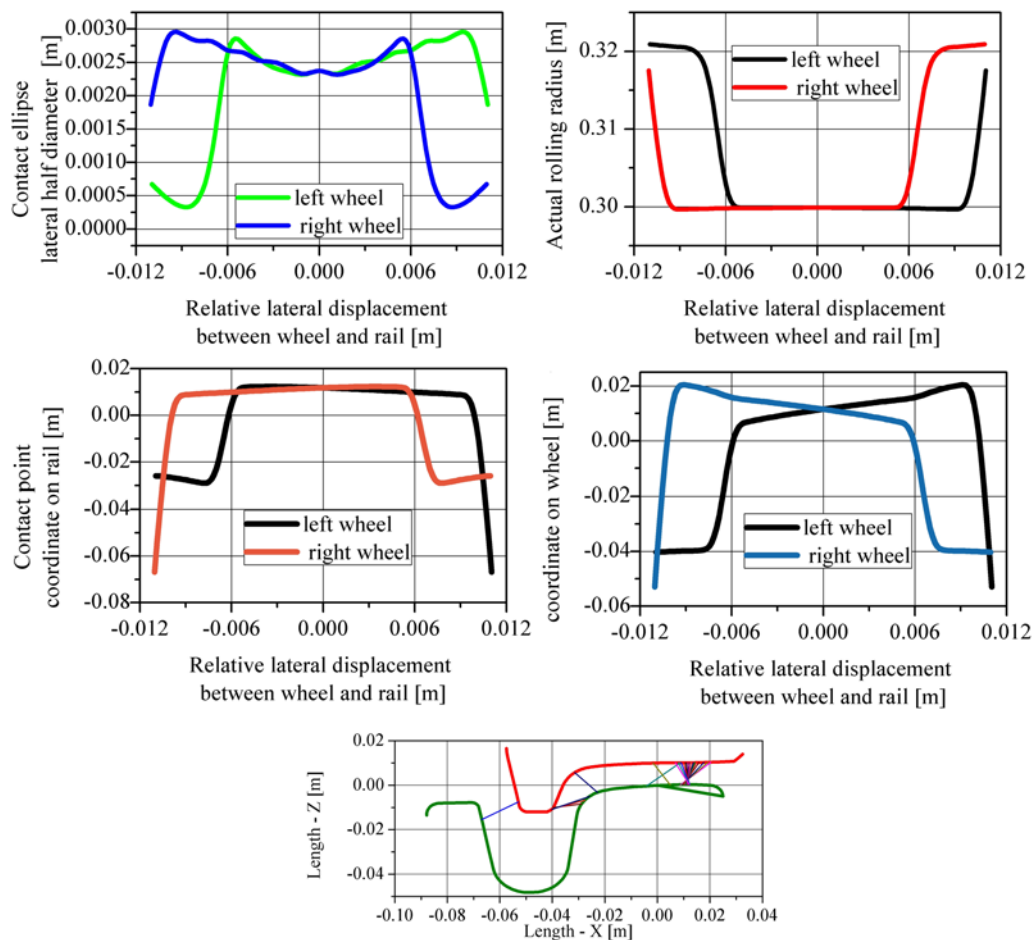

Fig. 6. Mutual positions of the wheel-rail profiles of the IRW tram with the PST wheel profile and the Ri60N rail profile with equivalent conicity of λ = 0.013 and lateral displacement of 3 mm

b/a	1	0.8	0.6	0.4	0.2	0.1
c_{11}	4.12	4.36	4.78	5.57	7.78	11.7
c_{22}	3.67	3.99	4.5	5.48	8.14	12.8
c_{23}	1.47	1.75	2.23	3.24	6.63	14.6
c_{33}	1.19	1.04	0.892	0.747	0.601	0.526

where: f_{11} is the lateral creep force coefficient, f_{12} denotes the lateral/spin creep force coefficient, f_{22} is the spin creep force coefficient, f_{33} describes the longitudinal creep force coefficient, and c_{ij} is the micro-slip coefficient [21] and the values of which are given in Table 1.

The above-described approach was chosen since the crank axis of the wheelset with independently rotating wheels may rotate relative to the vertical axis. It allows to determine the tangential forces in the wheel-rail contact zone, whereas the spin moment caused by the conicity of the wheel tread is taken into account.

For numerical tests using the adopted mathematical model of the vehicle, the nominal profile of the PST tram wheel was adopted. This profile is consistent with the standard [40]. According to technical guidelines included in the materials [46] grooved rails can be utilised in track curves with a radius under or equal to 150 m. Therefore, the Ri60N profile rail for the simulation was used. The positions of the wheel with the PST external profile in relation to the Ri60N rail was shown in Fig. 6.

3.3. Wheel drive control algorithms

Algorithms for controlling the operation of traction motors in trams equipped with IRW bogies have been the subject of many scientific publications [14, 3]. The control algorithm described in this paper was implemented to rail vehicle model by SIMAT module, which enables the co-simulation of MATLAB software, in which the algorithm was created, and the SIMPACK software, where the vehicle model was built. The calculation procedure is based on the fact that the angular velocities of independently rotating wheels of the vehicle's motor bogies are read in a single step while solving the equations of motion of the vehicle model. The angular velocities of the trailer bogie wheels are not processed due to the fact that they do not have any activators (motors) that could be controlled by the proposed algorithm. This is performed by the SIMAT module. This module transmits discrete values of the angular velocity of wheels ω_i to MATLAB software, where they are introduced to the control algorithm. The above mentioned velocities are compared in this algorithm with the set velocity ω_{set} of independently rotating wheels of the vehicle model. If a difference between their velocities occurs, i.e. when values of instantaneous velocities ω_i are lower than the defined velocity, the driving torque T transmitted to the particular wheel is changed.

For the simulated cases, some variants of controlling the motor torque T were used. In the first variant the driving torque was reduced to a minimum value of 0. In the second variant of the algorithm, where the braking process was taken into account, a negative braking torque of a given wheel was applied. In case when the angular velocity of a particular wheel exceeded nominal pre-set value, a negative braking torque was initiated. Previously determined value of the variable during data exchange (co-simulation) is transferred via SIMAT module to the tram model in the SIMPACK program to the appropriate actuator of the drive in a particular motor bogie.

The algorithm is repeated in the next calculation step until the simulation end time is reached. The general diagram of the traction motor drive control system using the MATLAB co-simulation with SIMAT and SIMPACK modules is shown in Fig. 7.

The topology of traction motors in tram bogies has significant impact on the wheel-rail contact forces. In order to verify it and deter-
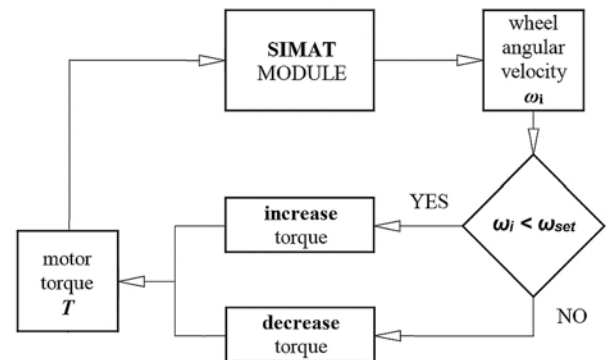
Fig 7. General wheel drive algorithm in bogies with IRW in the co-simulation software SIMPACK - MATLAB

mine the level of safety against derailment, three main configurations of torque distribution between traction motors of a given bogie were prepared. In the first configuration (marked as IRW-1), each of the four traction motors is controlled independently. The torque applied in one motor has no effect on the driving torque in other motors. In two subsequent configurations there is a group power supply of motors; for a group of two motors identical drive torques are applied. In this system, marked as IRW-2, the right or left group of wheels is supplied with the same torque. In the system marked as IRW-3, a group of wheels mounted on front or rear crank axles of a particular bogie is supplied.

Each control configuration was developed in two variants. The first one does not take into account wheel braking in the case when its angular velocity is higher than the defined velocity, while in the second it is taken into account. The simulation variants taking into account wheel braking have been marked with an additional "B" index.
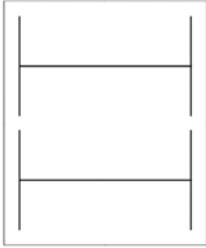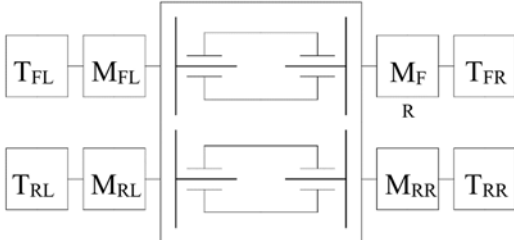
For a comparison with the classic wheelset, additional configuration of bogie with the same weight as the bogie with IRW was developed. The configuration - marked as "CWS" - is presented in Table 2 along with other configurations.

3.4. Description of testing methodology and simulation cases

To determine the level of safety against derailment of a railway vehicle it is necessary to measure the safety against derailment coefficient Y/Q (ratio of lateral force to vertical force of a particular wheel) and the leading wheel lift value D_z. Tests are performed on a track curve with a radius R = 150 m with a twisted section of 3‰, achieved by changing the height of the outer rail. Rails have the UIC60 profile. The guidelines for tests on safety against derailment of railway vehicles are set forth in standard EN 14363:2016 [10].

The validity of the safety against derailment test depends on the determined dry friction coefficient between the wheel and the rail. The test can be accepted if during a given run the measured friction coefficient is equal to or greater than 80% of the value of the previously determined dry friction coefficient μ_{dry}. The μ_{dry} coefficient depends on the value of the static vertical load of a particular wheel and on the attacking angle of a wheelset. Using the methodology from Annex A to EN 14363:2016 [10] and the above input data, the friction coefficient on dry rails μ_{dry} could be determined.

Table 2. Layouts of various motor drive systems of IRW bogies

symbol	layaout	description
CWS		classic wheelset in motor-bogies (for a comparison)
IRW-1 IRW-1B	T_{FL} M_{FL} M_{FR} T_{FR} T_{RL} M_{RL} M_{RR} T_{RR}	each of the traction motors powered separately
IRW-2 IRW-2B	T_L M_{FL} M_{FR} M_{RL} M_{RR} T_R	group power system for traction motors (right / left)
IRW-3 IRW-3B	T_F M_{FL} M_{FR} M_{RL} M_{RR} T_R	group power system for traction motors (front / back)
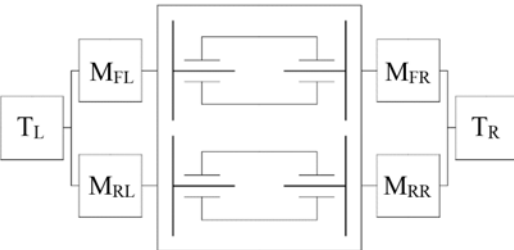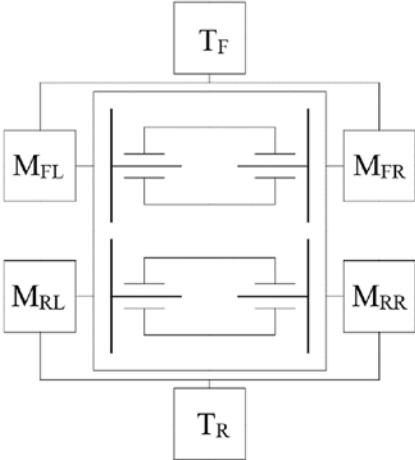
Usually the most unfavourable load state of a vehicle subject to the safety against derailment tests is tare condition, when vertical loads on particular wheels are the lowest. However, if the vehicle is equipped with suspension with a nonlinear characteristic, its influence on the obtained results should be determined. In order to increase the differences between vertical wheel loads in particular wheels standard EN 14363:2016 [10] demands that additional twist in the primary suspension should be introduced. This could be achieved by using steel shims.

Fig. 8 displays a cross-section of a wheel with the S1002 profile in critical (but still safe) position on the UIC60 profile rail. Both the wheel and the rail are in new, unused condition. The wheel contacts the rail at a point on the flange which connects straight section with a curved one. For such combination the distance between the wheel
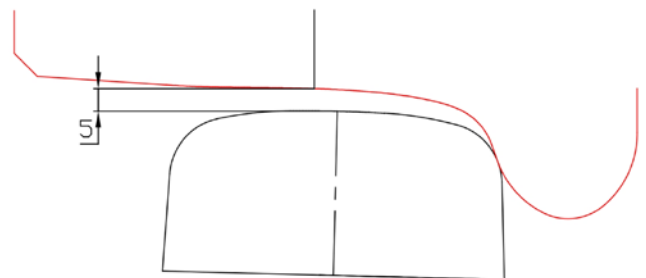

Fig. 8. Critical position of wheel profile S1002 on rail UIC 60 which defines the limit of wheel lift in safety against derailment test

tread at the point of the rolling circle and the rail surface is 5 mm. In standard EN 14363:2016 [10] it was adopted as the limit value for the wheel lift $D_{z,lim}$ for the safety against derailment tests on a twisted track curve.

Methods described in standard EN 14363:2016 [10] cannot be applied to tram vehicles. Compared to rail vehicles, trams are characterized by a much greater variety in kinematic systems of connections between carbodies and bogies. Tram vehicles mainly operate in cities and their infrastructure is adapted to local urban conditions, so in many cases it was necessary to plan track curves with a radius smaller than twisted track curve with a radius of R = 150 m, required in standard [10]. Results of the safety against derailment tests of a tram on such curve may not be critical.

The above-mentioned issues contributed to the development of a proprietary methodology for testing safety against derailment of tram vehicles on curves of tracks with different radii, which was first presented in article [19]. Based on document [46], which is the main handbook for designing tram infrastructure in Poland, the radius of curves to be used for simulation tests and the cant values for each of these curves were determined. The guidelines of the document [46] also define the inclination of the superelevation ramp equal to 1:300.

The curves with radii of 18, 25, 50 and 150 m were selected as representative for the tram infrastructure for the safety against derailment tests. To ensure operational safety as the most critical case, the inclination of the superelevation ramp equal to 1:150 was assumed (less favourable than in the document [46]); it corresponds to a track twist of approx. 6.67‰. At the exit of each of the analysed curves additional twist was added - the outer rail over a section of 6 m changed its height by 20 mm, which corresponds to 3.33‰ twist. Such geometrical parameters of the track curve are shown in Fig. 9. The total twist on each curve equals to 10‰ and corresponds to poor quality track infrastructure awaiting periodic renovation.

Rubber-metal elements with specific force-displacement characteristics dominate in the suspension systems of tram bogies. Stiffness of these elements depends both on atmospheric conditions (the lower the ambient temperature, the higher the stiffness in relation to the stiffness in the reference temperature) and manufacturing tolerance (usually +/- 15%). Therefore, it was decided to increase the nominal stiffness of all rubber-metal elements in the simulation model twice to ensure adequate level of safety against derailment also in conditions of low operating temperatures.

The nominal tram track gauge is 1435 mm, and the maximum - 1450 mm [46]. For the simulation purposes the range of rail gauge was extended to 1455 mm. In the above-mentioned range numerical simulations were carried out for cases of track gauge gradation every 5 mm. Assumed combinations of geometric parameters of the test tracks used for the proposed research method are presented in Table 3.

Table 3. Track geometry parameters for considered simulation cases

Curve radius [m]	Track twist on curve	Additional twist (outer rail)	Track gauge [m]
18,25,50,150	6.67‰	3.33‰	1.435; 1.440; 1.445; 1.450; 1.455

In order to reduce the length of the S-type track, and thus reduce the calculation time, the symmetry of the weight distribution to the right and left side of the tram was adopted. Thanks to it the level of safety against derailment could have been tested for only one direction of the track curve, i.e. the right one.

The key element of the developed research methodology for safety against derailment is the definition of a limit criterion for assessing the level of safety for particular tram. As already proved in the paper above, the decisive factor for the safety against derailment is the value of wheel lift D_z in relation to the top of rail. Wheel and rail profiles used for tram vehicles are completely different from those ones applied for railway vehicles. The outer profile of the rail was already mentioned before, i.e. Ri60N. Polish tram operators utilise trams mainly with two outer contours of wheels: T profile or PST. Their limit position on the Ri60N rail is shown in Fig. 10. The minimum wheel lift value achieved for T or PST profile combined with the Ri60N profile rail was D_z = 8.76 mm. Rounding
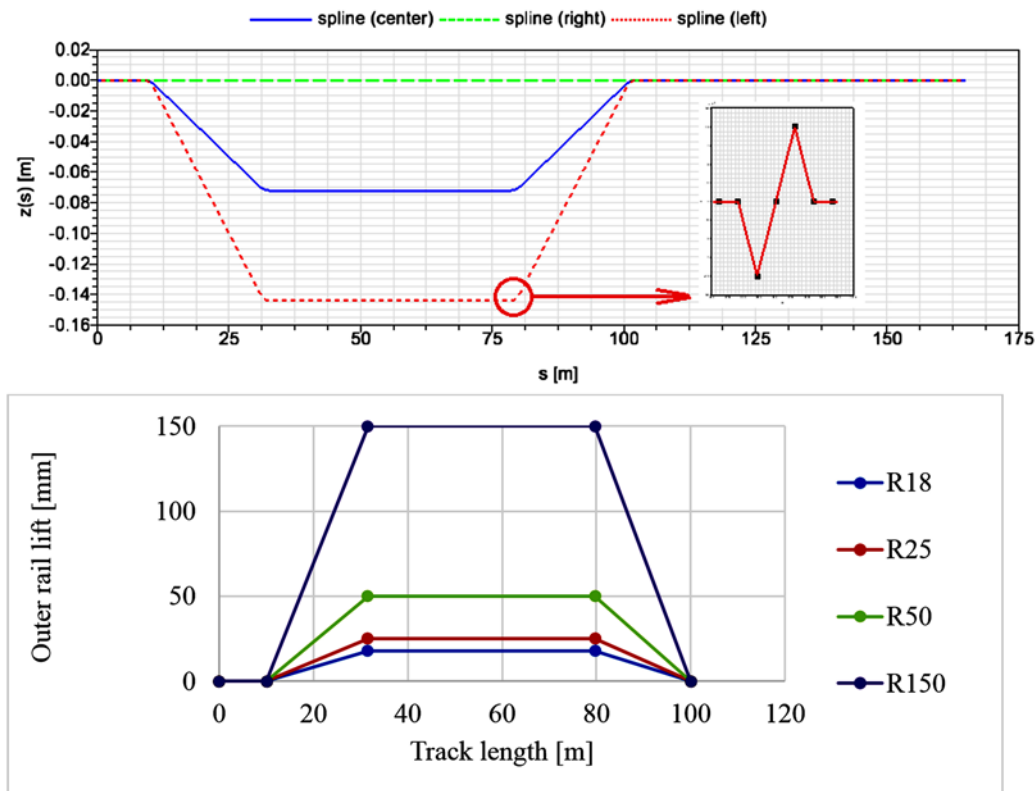

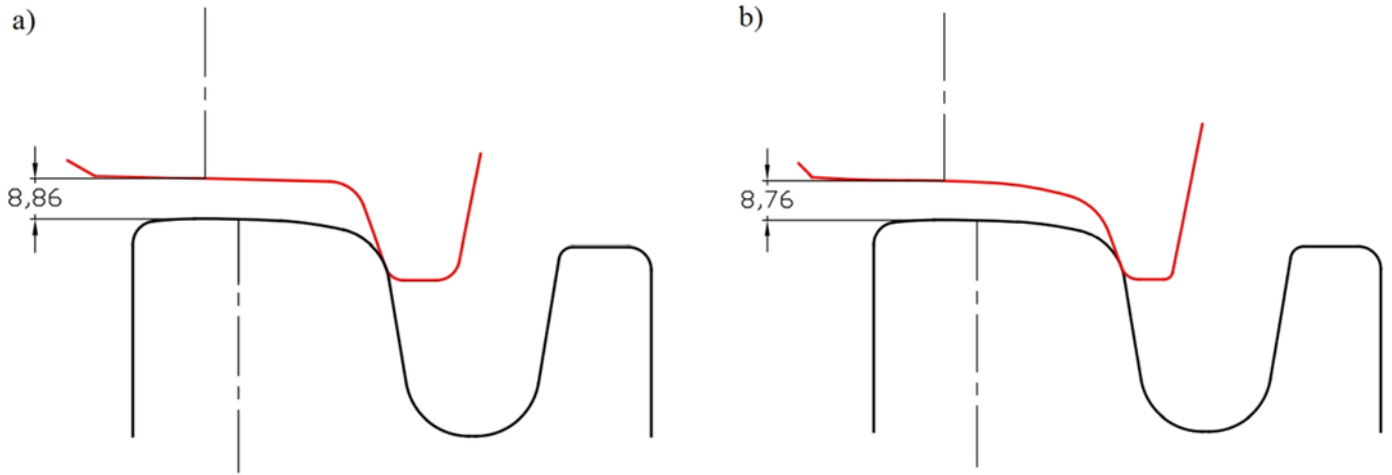*Fig. 9. A novel geometry of test track for proposed research methodology*

Fig. 10. Setting limit position of safety against derailment for wheels with profile T (a) or PST (b) with rail profile Ri60N

Table 4. List of parameters used for particular cases of developed test methodology

Steering algorithm	Curve radius [m]	Track gauge [m]
CWS, IRW-1, IRW-1B, IRW-2, IRW-2B, IRW-3, IRW-3B	18, 25, 50, 150	1.435; 1.440; 1.445; 1.450; 1.455

this value down to an integer, a higher level of safety against derailment can be obtained. Therefore, it is recommended that the value $D_{z,lim} = 8$ mm should be set as the limit value when determining the safety margin against derailment of tram vehicles. As to analysis of trams from other countries, a separate analysis should be performed for the wheel and rail profiles used there.

Table 4 includes parameters used for particular calculation cases, i.e. radius of curves, track gauges and variants of algorithms controlling the torque of traction motors. Results presented in the next chapter were obtained on the basis of simulation scenarios carried out with combinations of parameters from each of the columns in Table 4.

4. Results of numerical study

The result values of the wheel lift D_z of the front wheelset of the MB1 bogie for the left (FL) and right (FR) wheels obtained on the basis of the test results, were presented separately for each of the control algorithms used as a function of the curve radius and track gauge. Graphical representation with top values for wheel lift D_z is displayed in Tables 6-8. Moreover, signals of transverse wheel-rail contact forces for the leading wheel (left front) of MB1 bogie in the track curve with the assumed track gauge of 1435 mm were compared and presented in the graphs in Table 5. For the rear wheels of the MB1 bogie, regardless of analysed loadcase and the type of the assumed

Table 5. Charts of transverse wheel-rail Y contact forces for the leading wheel (front left) of the MB1 bogie in the right curve of the track with a track gauge of 1435 mm
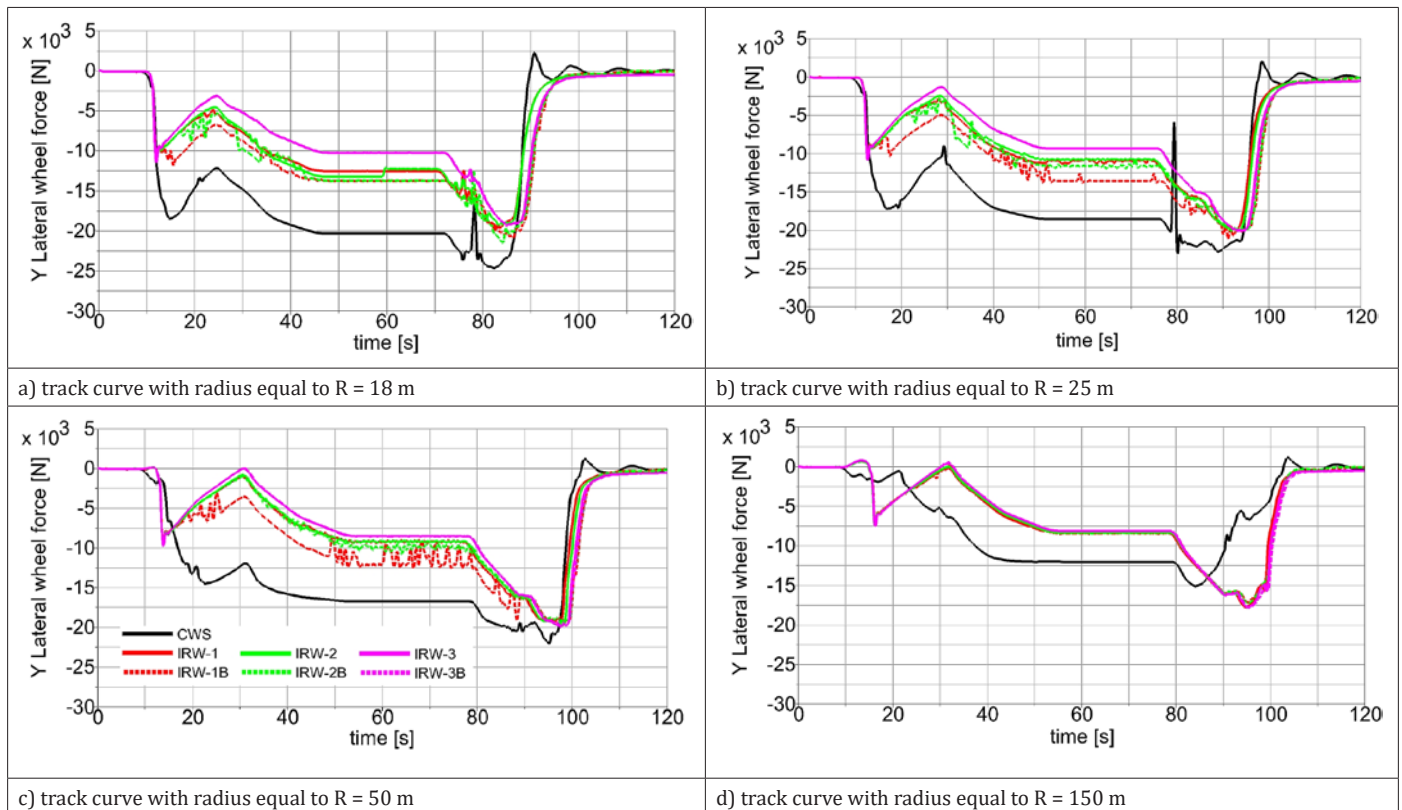

a) track curve with radius equal to R = 18 m

b) track curve with radius equal to R = 25 m

c) track curve with radius equal to R = 50 m

d) track curve with radius equal to R = 150 m

Table 6. *Graphical representation of the wheel lift Dz for a classic wheelset CWS*

Layout	Results [mm]										
CWS	CWS_MB1_FL						CWS_MB1_FR				
	R/s	**1435**	**1440**	**1445**	**1450**	**1455**	**R/s**	**1435**	**1440**	**1445**	**1450**	**1455**
	18	1.77	2.44	0	0	0	**18**	0	0	1.35	0	0
	25	3.76	4.71	0	0	0	**25**	0	0	0	0	0
	50	1.17	1.76	0	0	0	**50**	0	0	0	0	0
	150	0	0	0	0	0	**150**	0	0	0	0	0

drive control algorithm, their lift was equal to zero and therefore they are not presented in this summary. In the result Tables 6-8 the maximum values for a given wheel are marked in grey. In each of the numerical simulations loadcase the tram velocity was assumed as 1 m/s through the right curve of the track (Fig. 9) without a transition curve. In the geometric shape of the track, twist was assumed with a total value of 10‰, reflecting bad condition of maintenance. Based on the obtained results, the level of safety against derailment was defined by determining the vehicle wheel lift D_z during track curve negotiation. In all numerical simulations the vehicles had the same mass, including the movement simulation of bogies with standard wheelsets (CWS). Thanks to it an analogous signal of changes of vertical loads of tram wheels for an identical track system (regardless of the adopted control algorithm) could have been obtained.

For track gauge up to 1445 mm the front left wheel was mainly responsible for guiding bogie in the track. For larger track gauge values the lateral guidance in the track was taken over by the wheel on the inside of the curve, i.e. the right front wheel. This is reflected in the increase of Y/Q ratio for this wheel and for all analysed curve radii, as well as in the decrease of Y/Q ratio for the left front wheel. The reason for the above was the shape of the outer rail profile and rotation of bogie around its axis because, as confirmed by the papers [5, 27], the Ri60N profile applied in these tram simulation scenarios is grooved.

Lateral force applied to the guide wheel (known as the "guiding force" of rail vehicle wheel) in a standard wheelset is often greater than in an IRW bogie during entering and passing the curve, regardless of algorithm used. As the curve radius increases, the difference of guiding force value for standard wheelset loadcase and the loadcase of IRW bogie decreases. In a curve with radius R150 guiding forces for a bogie with IRW in the moment of entering and exiting the curve are greater than in the loadcase of a bogie with standard wheelset. No differences in the guiding force value resulting from the application of algorithms for controlling the operation of motor torque distribution in motor bogies with IRW can be found in curves up to R50 radius. Larger values can be achieved for IRW-1B and IRW-2B systems with motor braking. For IRW-3 and IRW-3B systems (corresponding to the group supply of the front-rear wheels drive), the force waveforms for each of the analysed curves were almost identical. As to curve with radius R150 no significant differences in the guiding force values can be identified, regardless of the applied torque control algorithm.

For all standard wheelset simulation loadcases the lowest values of wheel lift were obtained. The greatest wheel lift of the left front wheel (FL), equal to 4.71 mm, was achieved on a curve with a radius

R25 and a track gauge of 1440 mm, and the highest value for the right front wheel, equal to 1.35 mm, was obtained for a curve with a radius R18 and track width of 1445 mm. The results for the MB1 bogie from IRW turned out to be different. In all analysed loadcases, the highest values of the left front wheel (FL) lift were achieved on R50 curve with a track gauge of 1440 mm. The maximum value, i.e. 9.52 mm was obtained by applying the IRW-3 algorithm. The right front wheel (FR) reached maximum lift on R18 curve with a track gauge in the range of 1450-1455 mm. The highest value was achieved by using the IRW-2B algorithm. All values obtained for the front right wheel (FR) concerning the wheel lift on the rail groove matched the assumed limit $D_z \leq 8$ mm. The application of motor braking in the IRW control systems resulted in the reduction of maximum values of the left front wheel lift (running in the right curve) from 9.25 mm to 7.33 mm, from 9.50 mm to 9.32 mm, and from 9.52 mm to 7.82, corresponding with the variant of algorithm IRW-1, IRW-2 and IRW-3.

5. Summary

Based on numerical tests of the light rail vehicle model with independently rotating wheels, very high sensitivity of trajectory of this vehicle motion caused by the method of controlling the vehicle's wheel drive has been identified.

According to the results of papers [12, 44] describing the dynamics of rail vehicles with independently rotating wheels, the effect of unstable bogie in the central position of the track was observed. Such cases occurred only in the absence of wheel drive control, as opposed to correct vehicle stabilization in the axis of track for bogies with standard wheelsets [17, 42]. This instability effect influences the value of contact forces between wheel flanges and rail head adversely. Such phenomena deteriorate technical conditions of operation and increase maintenance costs of the rolling stock [6, 38, 49].

It should be also pointed out that the drive control system with the option of braking wheels with the motor - proposed by the authors - allows to reduce angular velocity differences between individual wheels. An induced speed reduction of a given wheel increases the forces of lateral interaction with the track. This, consequently, leads to a slight growth of the lateral force Y relative to control systems without the braking option. Bearing this in mind, a conclusion can be drawn that this phenomenon reduces wheel lift and improves both operating conditions and driving safety. This is one of the ways in designing an effective stabilizing control. Authors proved that, regardless of selected drive and braking control system, the determined

Table 7. *Graphical representation of the wheel lift Dz with various control algorithms of IRW without wheels motor braking*

Layout	Results [mm]										

IRW-1

IRW-1_MB1_FL

IRW-1_MB1_FR

R/s	1435	1440	1445	1450	1455	R/s	1435	1440	1445	1450	1455
18	0	0	0	0	0	18	0	0	1.75	4.38	4.05
25	3.44	4.35	0	0	0	25	0	0	0	0	0
50	8.82	9.25	0	0	0	50	0	0	0	0	0
150	1.37	1.25	0	0	0	150	0	0	0	0	0

IRW-2

IRW-2_MB1_FL

IRW-2_MB1_FR

R/s	1435	1440	1445	1450	1455	R/s	1435	1440	1445	1450	1455
18	0	0	0	0	0	18	0	0	1.77	4.48	3.77
25	4.02	4.65	0	0	0	25	0	0	0	0	0
50	9.41	9.50	0	0	0	50	0	0	0	0	0
150	1.37	1.26	0	0	0	150	0	0	0	0	0

IRW-3

IRW-3_MB1_FL

IRW-3_MB1_FR

R/s	1435	1440	1445	1450	1455	R/s	1435	1440	1445	1450	1455
18	0	0	0	0	0	18	0	0	1.88	2.72	4.13
25	4.18	4.83	0	0	0	25	0	0	0	0	0
50	9.34	9.52	0	0	0	50	0	0	0	0	0
150	1.37	1.25	0	0	0	150	0	0	0	0	0

values of guiding forces Y of tram wheels with IRW for all analysed radii curves of the track were smaller than in the similar vehicle with standard wheelsets. The greater the difference in the value of leading force between the analysed vehicles (standard wheelset and IRW), the smaller the curve radius of the track used for simulations. This proves the advisability of further development of the IRW bogie structure which allows for the reduction of wheel-rail transverse impacts on the urban track infrastructure, where many curves have radius smaller than R = 150 m (e.g. on tram loops). Additional positive aspect of

Table 8. Graphical representation of the wheel lift Dz with various control algorithms of IRW with wheels motor braking

Layout	Results [mm]										

IRW-1B

IRW-1B_MB1_FL

IRW-1B_MB1_FR

R/s	1435	1440	1445	1450	1455	R/s	1435	1440	1445	1450	1455
18	0	0	0	0	0	18	0	0	1.74	2.78	4.13
25	4.43	4.66	0	0	0	25	0	0	0	0	0
50	6.96	7.33	0	0	0	50	0	0	0	0	0
150	0	0	0	0	0	150	0	0	0	0	0

IRW-2B

IRW-2B_MB1_FL

IRW-2B_MB1_FR

R/s	1435	1440	1445	1450	1455	R/s	1435	1440	1445	1450	1455
18	0	0	0	0	0	18	0	0	1.74	4.45	4.29
25	4.68	5.24	0	0	0	25	0	0	0	0	0
50	9.11	9.32	0	0	0	50	0	0	0	0	0
150	0	0	0	0	0	150	0	0	0	0	0

IRW-3B

IRW-3B_MB1_FL

IRW-3B_MB1_FR

R/s	1435	1440	1445	1450	1455	R/s	1435	1440	1445	1450	1455
18	0	0	0	0	0	18	0	0	1.80	2.71	4.06
25	3.77	4.54	0	0	0	25	0	0	0	0	0
50	7.60	7.82	0	0	0	50	0	0	0	0	0
150	1.03	0	0	0	0	150	0	0	0	0	0

the lower lateral force Y in the wheel-rail contact is the reduction of noise level.

The analysis of the obtained results showed that vehicles with independently rotating wheels should be carefully designed along with the drive control system in order to minimize the lift and wear of wheels.

The introduction of bogies with independently rotating wheels of the IRW type to tram vehicles is a step forward in the development of the design of modern chassis of such vehicles. They ensure greater driving comfort for passengers and, thanks to proper drive control

systems, forces of the lateral interaction of the wheel with the rail and can be reduced, which consequently, slows down the track wear.

The study results presented in this paper may be helpful in the processes of designing tram vehicles and their drive control systems. They can also be useful for their users and operators who are respon-sible for the reliability and maintenance of the rolling stock of tram vehicles with independently rotating wheels. This is of particular importance since the number of variants of tram structures with the drive system under consideration will grow in the near future due to their operational advantages.

References

1. Bogacz R, Konowrocki R. On new effects of wheel-rail interaction. Archive of Applied Mechanics 2012; 82: 1313-1323, https://doi.org/10.1007/s00419-012-0677-6.
2. Cho Y. Verification of control algorithm for improving the lateral restoration performance of an independently rotating wheel type railway vehicle. International Journal of Precision Engineering and Manufacturing 2020; 21: 247-1258, https://doi.org/10.1007/s12541-020-00346-4.
3. Chudzikiewicz A, Firlik B. Light rail vehicle dynamics from a running safety perspective Archives of Transport 2009; 21: 39-49.
4. Chudzikiewicz A, Sowińska M, Krzyżyński T, Maciejewski I. Modeling of wheel set movement with independently rotating wheels including the wheel control system. Logistyka 2015; 4: 32-139.
5. Chudzikiewicz A, Sowiński B. Modelling and simulation of trams bogies with fully independently rotating wheels. Dynamics of vehicles on roads and tracks 2016; 1427-1434, https://doi.org/10.1201/b21185-151.
6. Chudzikiewicz A, Korzeb J. Simulation study of wheels wear in low-floor tram with independently rotating wheels. Archive of Applied Mechanics 2018; 88: 75-192, https://doi.org/10.1007/s00419-017-1301-6.
7. Chudzikiewicz A, Sowińska M. Modelling and simulations of dynamics of the low-floor tramcar with independently rotating wheels. Communications - Scientific Letters of the University of Zilina 2017; 17 (4): 45-52.
8. Goodall RM and Mei TX. Mechatronic strategies for controlling railway wheelsets with independently rotating wheels, in Proceedings of the IEEE/ASME International Conference on Advanced Intelligent Mechatronics, 2005; 1: 225-230, https://doi.org/10.1109/AIM.2001.936458.
9. Guerrieri M. Tramways in urban areas an overview on safety at road intersections. Urban Rail Transit 2018; 4: 223-233, https://doi.org/10.1007/s40864-018-0093-5.
10. EN 14363:2016 - Railway applications - Testing and Simulation for the acceptance of running characteristics of railway vehicles - Running behaviour and stationary tests.
11. Firlik B, Staśkiewicz T, Jaśkowski W, Wittenbeck L. Optimisation of a tram wheel profile using a biologically inspired algorithm Wear, 2019; 430-431: 12-24, https://doi.org/10.1016/j.wear.2019.04.012.
12. Hauser V, Nozhenko O, Kravchenko K, Loulová M, Gerlici J, Lack T. Proposal of a steering mechanism for tram bogie with three axle boxes. Procedia Engineering 2017; 192 (41): 289-294, https://doi.org/10.1016/j.proeng.2017.06.050.
13. Gill A, Firlik B, Kobaszynska-Twardowska A. Analysis of the Distribution of Passengers inside a Tram, in J. Pombo, (Editor), Proceedings of the Third International Conference on Railway Technology: Research, Development and Maintenance", Civil-Comp Press, Stirlingshire, UK, Paper 303, 2016.
14. Grether G, Looye G, Heckmann A. Lateral guidance of independently rotating wheel pairs using feedback linearization, Proceedings of the Fourth International Conference on Railway Technology: Research, Development and Maintenance, Spain, 2018.
15. Hoshi M, Ookubo Y, Murakami N, Arai T, Kono H, Aruga H. Development of bogie for user friendly, extra low floor, light rail vehicle (LRV) using independent wheel system and next generation LRV, Mitsubishi Heavy Industries Ltd., Technical Review 2007; 44 (2): 1-4.
16. https://lucchinirs.com/wp-content/uploads/2017/05/limoset-1.jpg (access on 07.07.2020).
17. Iwnicki S. Handbook of railway vehicle dynamics. CRC Press. 2006, https://doi.org/10.1201/9781420004892.
18. Ji Y, Ren L, Zhou J. Boundary conditions of active steering control of independent rotating wheelset based on hub motor and wheel rotating speed difference feedback. Vehicle System Dynamics 2018; 56 (12): 1883-1898, https://doi.org/10.1080/00423114.2018.1437273.
19. Kalinowski D, Szolc T, Konowrocki R. The new simulation approach of tramway safety against derailment evaluation in term of vehicle dynamics. Transbaltica XI: Transportation Science and Technology, Vilnius (LT), 2020: 245-254, https://doi.org/10.1007/978-3-030-38666-5_26.
20. Kalker JJ. Review of wheel - rail rolling contact theories. The general problem of rolling contact. Eds. A.L. Browne and N.T. Tsai. Vol. 40. New York: American Society of Mechanical Engineers, 1980.
21. Kalker JJ. A strip theory for rolling contact of two elastic bodies in presence of dry friction. Ph. D. dissertation, Delft University of Technology, 1976.
22. Klamka J, Grzesiak R. Drive bogie for low-floor rail vehicle (Wózek napędowy do niskopodłogowego pojazdu szynowego), Patent PL225456, 28.04.2017 WUP 04/17.
23. Kolar J. Modern trends in the drive wheelsets of rail vehicles. In: Dynybyl V., Berka O., Petr K., Lopot F., Dub M. (eds) The Latest Methods of Construction Design. Springer, Cham, 2016: 27-35, https://doi.org/10.1007/978-3-319-22762-7_5.
24. Konowrocki R, Bajer Cz. Friction rolling with lateral slip in rail vehicles. Journal of Theoretical and Applied Mechanics 2009; 47 (2): 275-293.
25. Konowrocki R, Bogacz R. Tram vehicles with independently rotating wheels, chapter: Overview of light rail vehicle solutions used in operation, Book Warsaw University of Technology Publishing House 2019: 148-164, ISBN: 978-83-8156-010-8 (in Polish).
26. Konowrocki R, Chojnacki A. Analysis of rail vehicles' operational reliability in the aspect of safety against derailment based on various methods of determining the assessment criterion Eksploatacja i Niezawodnosc - Maintenance and Reliability 2020; 22 (1): 73-85, https://doi.org/10.17531/ein.2020.1.9.
27. Konowrocki R. Tram vehicles with independently rotating wheels, chapter: Simulations of tram vehicle dynamics with respect to different operating conditions, Warsaw University of Technology Publishing House 2019: 297-328, ISBN: 978-83-8156-010-8 (in Polish).
28. Liang B, Iwnicki S D. An experimental study of independently rotating wheels for railway vehicles. International Conference on Mechatronics and Automation, Harbin, 2007: 2282-2286, https://doi.org/10.1109/ICMA.2007.4303908.
29. Liang B, Iwnicki S D. Independently rotating wheels with induction motors for high-speed trains. Journal of Control Science and Engineering 2011: 1-7, https://doi.org/10.1155/2011/968286.

30 Li H, Chi M, Liang S, Wu X. Curve-passing performance of independent rotating wheels based on differential feedback. Journal of Vibration and Shock 2018; 37 (23): 126-132, https://doi.org/10.13465/j.cnki.jvs.2018.23.018.

31. Lindblom J. Trackbound vehicle with steering of wheel axles, Patent EP0939717A1, 1999.

32. Lu ZG, Sun XJ, Yang JQ. Integrated active control of independently rotating wheels on rail vehicles via observers. Journal of Rail and Rapid Transit 2017; 231 (3): 295-305, https://doi.org/10.1177/0954409716629705.

33. Macián V, Tormos B, Herrero J. Maintenance management balanced scorecard approach for urban transport fleets. Eksploatacja i Niezawodnosc - Maintenance and Reliability, 2019, 21 (2): 226-236, https://doi.org/10.17531/ein.2019.2.6.

34. Matej J, Seńko J, Awrejcewicz J. Dynamic properties of two-axle freight wagon with uic double-link suspension as a non-smooth system with dry friction. In: Awrejcewicz J. (eds) Applied Non-Linear Dynamical Systems. Springer Proceedings in Mathematics & Statistics 2014; 93: 255-268, https://doi.org/10.1007/978-3-319-08266-0_18.

35. Mei T X, Goodall R M. Practical strategies for controlling railway wheelsets independently rotating wheels. Journal of Dynamic Systems, Measurement and Control, Transactions of the ASME, 2003; 125 (3): 354-360, https://doi.org/10.1115/1.1592191.

36. Michajłow M, Jankowski Ł, Szolc T, Konowrocki R. Semi-active reduction of vibrations in the mechanical system driven by an electric motor. Optimal Control Applications & Methods 2017; 38 (6): 922-933, https://doi.org/10.1002/oca.2297.

37. Myamlin S, Kirilchuk O, Metyzhenko V. Mathematical model of wheelset oscillations with independent wheel rotation in the horizontal plane. Science and Transport Progress 2016; 4 (64): 134-141, https://doi.org/10.15802/stp2016/77999.

38. Opala M. Study of the derailment safety index Y/Q of the low-floor tram bogies with different types of guidance of independently rotating wheels. Archives of Transport 2016; 38 (2): 39-47, https://doi.org/10.5604/08669546.1218792.

39. Opala M. Evaluation of bogie centre bowl friction models in the context of safety against derailment simulation predictions. Archive of Applied Mechanics 2018; 88 (6): 943-953, https://doi.org/10.1007/s00419-018-1351-4.

40. PN-K-92016:1997 - Tram wheel sets, flexible - Surfaced tyres - Requirements and testings.

41. Polach O. A fast wheel-rail forces calculation computer code. Vehicle System Dynamics 1999; 33: 728-739, https://doi.org/10.1080/00423114.1999.12063125.

42. Shabana AA, Zaazaa KE, Sugiyama H. Railroad vehicle dynamics : a computational approach. CRC Press 2008, https://doi.org/10.1201/9781420045857.

43. Staśkiewicz T, Firlik B.Verification of a tram wheel new profile dynamic behavior. Journal of Mechanical and Transport Engineering 2017; 69 (1): 49-60, https://doi.org/10.21008/j.2449-920X.2017.69.1.05.

44. Suda Y, Wang W, Nishina M, Lin S, Michitsuji Y. Self-steering ability of the proposed new concept of independently rotating wheels using inverse tread conicity. Vehicle System Dynamics 2012; 50: 291-302, https://doi.org/10.1080/00423114.2012.672749.

45. Tabaszewski M, Firlik B. Assessment of the track condition using the Gray Relational Analysis method. Eksploatacja i Niezawodnosc - Maintenance and Reliability 2018; 20 (1): 147-152, https://doi.org/10.17531/ein.2018.1.19.

46. Technical guidelines for the design and maintenance of tram tracks, Ministry of Administration, Local Economy and Environmental Protection, Department of Public Transport and Roads, Warsaw 1983.

47. Transport in the European Union - current trends and issues, Report European Commission, Directorate-General Mobility and Transport, B-1049 Brussels, March 2019.

48. UIC 518, Testing and approval of railway vehicles from the point of view of their dynamic behaviour - Safety - Track fatigue - Ride quality 2009.

49. Wijata X, Awrejcewicz A, Matej J, Makowski M. Mathematical model for two-dimensional dry friction modified by dither. Mathematics and Mechanics of Solids 2017; 2 (10): 1936-1949, https://doi.org/10.1177/1081286516650483.

50. Zirek A, Voltr P, Lata M. Validation of an anti-slip control method based on the angular acceleration of a wheel on a roller rig. Proceedings of the Institution of Mechanical Engineers, Part F: Journal of Rail and Rapid Transit 2020; 234 (9): 1029-1040, https://doi.org/10.1177/0954409719881085.